

EXTREMUM SEEKING

FOR WIND AND SOLAR ENERGY APPLICATIONS

BY AZAD GHAFFARI, MIROSLAV KRSTIC AND SRIDHAR SESHAGIRI

Extremum seeking (ES) was invented in 1922 and is one of the oldest feedback methods. Rather than regulation, its purpose is optimization. For this reason, applications of ES have often come from energy systems. The first noted publication on ES in the West is Draper and Li's application to spark timing optimization in internal combustion engines¹. In the ensuing decades, ES has been applied to gas turbines and even nuclear fusion reactors. Renewable energy applications have brought a new focus on the capabilities of ES algorithms. In this article we present applications of ES in two types of energy conversion systems for renewable energy sources: wind and solar energy. The goal for both is maximum power point tracking (MPPT), or, the extraction of the maximum feasible energy from the system under uncertainty and in the absence of a priori modeling knowledge about the systems. For the wind energy conversion system (WECS), MPPT is performed by tuning the set point for the turbine speed using scalar ES. Performing MPPT for the photovoltaic (PV) array system entails tuning the duty cycles of the DC/DC converters employed in the system using multivariable ES. Experimental results are provided for the photovoltaic system.

Increasing availability of energy storage devices intensifies the effort to harvest maximum power from renewable sources, particularly wind turbines (WT) and PV systems. Renewable sources operate under a wide range of uncertain environmental parameters and disturbances. For example, uncertain quantities such as wind speed in WT and solar irradiance in PV modules affect the respective power maps and the maximum power points (MPP). The power map is also a function of a control input—the turbine speed in WT and the terminal voltage in the PV modules. The power map of a WT has a unique MPP with respect to turbine speed at each level of wind speed. Likewise, the power map of a PV module has a unique MPP with respect to terminal voltage at each level of solar irradiance.

The process of governing a WT or PV module to its MPP is known as maximum power point tracking (MPPT). The conventional perturb and observe (P&O) techniques do so by a combination of adding a step perturbation to the control signal and monitoring the direction of changes in power². Most techniques derived from P&O are based on discrete analysis and require a delicate balance between the amplitude of the control input step perturbation and the possible changes in environmental parameters. Moreover, the sampling frequency needs to be carefully selected with respect to the response time of the system to the step perturbation. Since the system is not linear, the sampling frequency is also a function of the step size and of the magnitude of changes in environmental parameters.

Extremum seeking is an attractive alternative to P&O techniques for solving MPPT problems in wind and solar systems. As a model-free, real-time optimization approach, ES is well suited for systems with unknown dynamics or those that are affected by high levels of uncertainty or external dynamics, like WT and PV systems. Similar to P&O techniques, ES employs perturbations. However, instead of employing a discrete step perturbation, ES uses a

continuous oscillatory perturbation, also known as a “probing function.” More importantly, ES does not merely monitor the direction of the output response but exploits the measured response to estimate the gradient of the power map and update the control input in proportion to the gradient of the power map₃₋₆.

ES has the dual benefit of rigorously provable convergence and the simplicity of hardware implementation. In addition to a probing signal, the ES algorithm employs only an integrator, as well as optional high-pass and a low-pass filters. The amplitude and frequency of the probing function in ES influence the precision of the MPPT algorithm. However, the frequency selection is not as complicated as the selection of the sampling frequency in P&O technique. For dynamic systems, it is enough to select the ES probing frequency reasonably smaller than the highest frequency that can pass the system without significant attenuation.

ES guides the system to its MPP regardless of changes in environmental parameters, as long as the changes are slow. While the power map shape defines the convergence rate of the conventional gradient-based ES, we also present in this article more sophisticated schemes like the Newton-based ES to alleviate the issue of unsymmetrical transients₇.

In some cases we need an inner-loop control to achieve desired closed-loop performance, for example, for speeding up the convergence rate and alleviating magnetic saturation

in WT systems. Combining a discrete MPPT method such as P&O with a continuous inner-loop control creates a hybrid system that needs careful parameter selection, particularly the sampling period and perturbation amplitude. In contrast, ES can be applied without modifications to any system with a stabilizing inner-loop control.

A distributed MPPT architecture is not the most efficient option for handling a multivariable power map, such as a cascade PV configuration with one converter per module. For multivariable MPPT, the complexity of P&O algorithms increases dramatically with the size of the input vector. In contrast, ES trivially extends to multivariable MPPT, with only a few restrictions in selecting the probing frequencies. Furthermore, with ES we have the option of employing the algorithm’s Newton-based version to achieve transients that are symmetric relative to the peak of the MPP and uniform in speed for multiple modules.

This paper is organized as follows. The next section introduces both gradient and Newton-based ES schemes. Subsequently, a Scalar gradient-based ES is combined with a nonlinear inner-loop control developed from field-oriented control (FOC) to achieve power control and optimization in WT. Simulation results demonstrate the effectiveness of the proposed algorithm. Finally, multivariable MPPT based on ES for PV systems are presented, and the validity of the proposed algorithms with experimental results are verified.

THE BASICS OF EXTREMUM SEEKING

A gradient-based ES for multi-input static maps is shown in **Figure 1**. The algorithm measures the scalar signal $y(t) = Q(\theta(t))$, where $Q(\cdot)$ is an unknown map whose input is the vector $\theta = [\theta_1, \theta_2, \dots, \theta_n]^T$. The map has a unique maximum point at $\theta^* = [\theta_1^*, \theta_2^*, \dots, \theta_n^*]^T$ where

$$\frac{\partial Q}{\partial \theta}(\theta^*) = 0, \quad \frac{\partial^2 Q}{\partial \theta^2}(\theta^*) = H < 0, \quad H = H^T \quad 1$$

where H is the Hessian matrix and defines the shape of the unknown map around its maximum point.

Gradient estimation is helped by the signals

$$S(t) = [a_1 \sin(\omega_1 t) \cdots a_n \sin(\omega_n t)]^T \quad 2$$

$$M(t) = \left[\frac{2}{a_1} \sin(\omega_1 t) \cdots \frac{2}{a_n} \sin(\omega_n t) \right]^T \quad 3$$

with nonzero perturbation amplitudes a_i and with a gain matrix K that is diagonal. Some restrictions are imposed on the probing frequencies, ω_i . For the unknown map, $Q(\cdot)$, the averaged system is

$$\dot{\hat{\theta}} = KH\hat{\theta} \quad 4$$

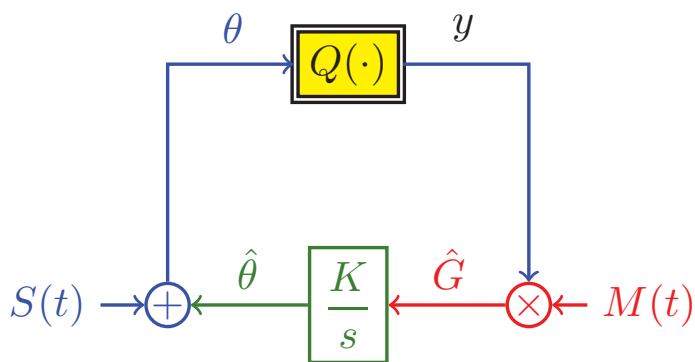


FIGURE 1 The gradient-based ES for a static map.

where $\hat{\theta}$ is an estimate of the optimal input vector. If the user chooses the elements of the diagonal gain matrix K as positive, the ES algorithm is guaranteed to be locally convergent. However, the convergence rate depends on the unknown Hessian H . This weakness of the gradient-based ES algorithm is removed with the Newton-based ES algorithm.

A Newton version of the ES algorithm, shown in **Figure 2**, ensures that the convergence rate be user-assignable, rather

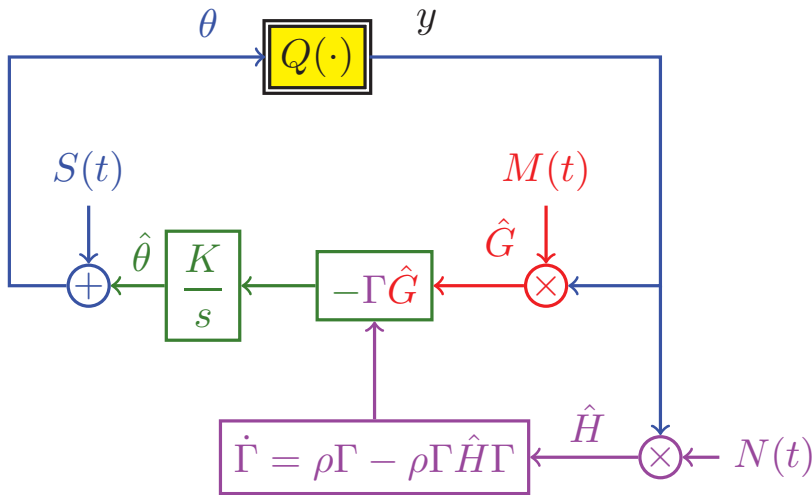


FIGURE 2 A Newton-based ES for a static map.

than being dependent on the unknown Hessian of the map₇. The elements of the demodulating matrix $N(t)$ for generating the estimate of the Hessian are given by

$$N_{ii}(t) = \frac{16}{a_i^2} \left(\sin^2(\omega_i t) - \frac{1}{2} \right), N_{ij}(t) = \frac{4}{a_i a_j} \sin(\omega_i t) \sin(\omega_j t). \quad 5$$

The multiplicative excitation helps to generate the estimate of the Hessian as $\hat{H}(t) = N(t)y(t)$. The Riccati matrix differential equation $\dot{\Gamma}(t)$ generates an estimate of the Hessian's inverse matrix, avoiding matrix inversions of Hessian estimates that may be singular during the transient.

A quadratic map's averaged system in error variables $\tilde{\theta} = \hat{\theta} - \theta^*$, $\tilde{\Gamma} = \Gamma - H^{-1}$ is

$$\frac{d\tilde{\theta}}{dt} = -K\tilde{\theta}, \quad \frac{d\tilde{\Gamma}}{dt} = -\rho\tilde{\Gamma}. \quad 6$$

Because they are determined by K and ρ , the eigenvalues are independent of the unknown H . As a result, the (local) convergence rate is user-assignable.

ES extends in a relatively straightforward manner from static maps to dynamic systems, provided the dynamics are stable and the parameters of the algorithm are chosen so that the dynamics are slower than those of the plant.

In the following section, the scalar gradient-based ES is applied to MPPT of a wind energy conversion system (WECS), with an inner-loop control.

WIND ENERGY CONVERSION SYSTEMS

Wind turbines work in four different regions (see **Figure 3**). Available wind power on the blade impact area is defined as

$$P_w = 2\rho_a A V_w^3, \quad A = \pi R^2, \quad 7$$

where R is the blade length, ρ_a is air density, and V_w is wind speed.

For Region II MPPT the turbine power is related to the wind power as

$$P_t = \omega_t T_t = C_p(V_w, \omega_t) P_w, \quad 8$$

where T_t is the rotor torque, ω_t is the turbine speed, and C_p is the non-dimensional power coefficient, which is a measure of the ratio of the turbine power to the wind power.

The turbine speed can be used to change the power coefficient, C_p , which results in power control and optimization. The MPPT algorithm in sub-rated power region should be able to guide the WT to its MPP regardless of the variations of the wind speed. The power captured by the WT is defined by the wind speed, V_w , and the turbine speed, ω_t . The wind speed is a disturbance input and the turbine speed can be manipulated to govern the turbine power to its MPP in sub-rated region. The variation of turbine power versus turbine speed is shown in **Figure 4** for different wind speeds. As shown in Fig. 4, under a constant wind speed the relevant power curve has a unique MPP, which is defined by a specific turbine speed.

Inner-Loop Control Design for WECS

One can manipulate the stator voltage amplitude, V_{om} , and its frequency, ω_o , to obtain the desired closed-loop performance for WECS. We introduce an integrator

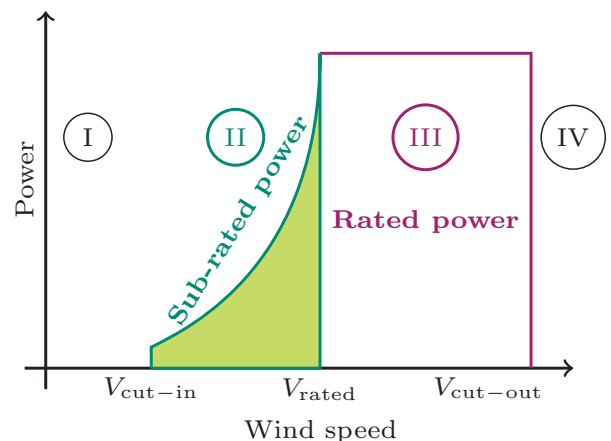


FIGURE 3 Typical power curve of WT including four operating regions.

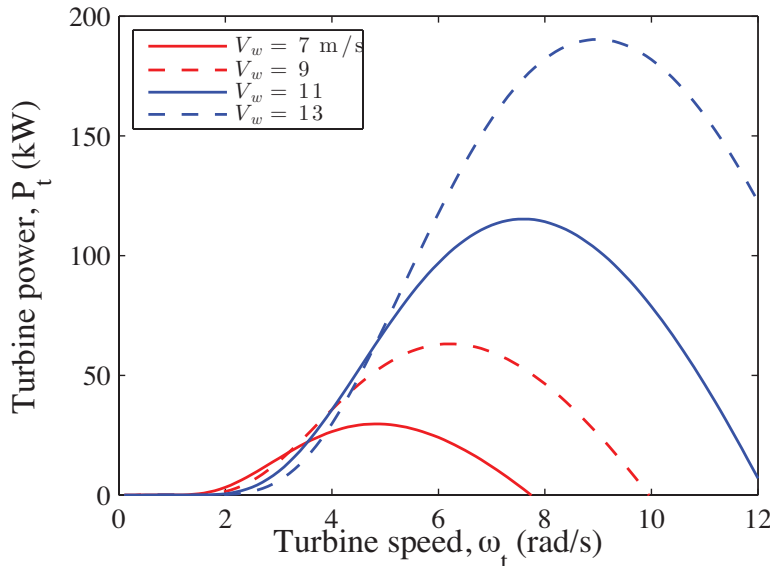


FIGURE 4 Variation of the turbine power versus turbine speed for different wind speeds.

and an auxiliary input, u_2 , to achieve input-output decoupling in WECS dynamics. Using one step of integration in front of V_{om} the extended equations of WECS are introduced as follows:

$$\dot{x} = f(x) + g_1 u_1 + g_2 u_2, \quad x \in \mathbb{R}^9, \quad u \in \mathbb{R}^2 \quad 9$$

where $x = [i_\alpha, i_\beta, \lambda_\alpha, \theta_o, V_{om}, \omega_r, \tilde{\theta}, \omega_t]^T$ where i_α and i_β are stator currents, λ_α and λ_β are rotor fluxes, $\tilde{\theta} = \theta_t - \frac{\theta_r}{p_m}$, $\theta_r = \int_0^t \omega_r dt$, ω_r is the rotor electrical frequency, $u_1 = \omega_o$ is the electrical frequency of the stator, u_2 is an auxiliary input (voltage amplitude rate) which generates the voltage amplitude of the stator.

As seen in Fig. 4, turbine speed controls power generation. Decoupling the rotor flux and electromagnetic torque produces the benefit of field-oriented control (FOC). Turbine speed, x_9 , and flux amplitude, $x_3^2 + x_4^2$, are introduced as measurable outputs for this reason. Feedback linearization is applied based on the selected outputs. This results in the regulation of turbine speed, ω_t , to its reference value ω_t^{ref} , while the amplitude of rotor flux, $|\lambda| = \sqrt{x_3^2 + x_4^2}$, converges to its desired value, $|\lambda|^{\text{ref}}$.

Wind Turbine Power Optimization

To overcome challenges associated with the conventional power control and optimization algorithms and to remove the dependence of the MPPT algorithm on system modeling and identification, an ES algorithm for MPPT of WECS is employed.

Access to turbine power measurements and speed manipulation are assumed in this article. Although there is no model of the power coefficient or turbine power, its power map has one MPP under any wind speed.

The proposed nonlinear control not only achieves the desired closed-loop performance, but faster response time (high power efficiency) as it also prevents magnetic saturation. The ES scheme with inner-loop control

is shown in **Figure 5**. Shown here, the reference inputs of the inner-loop control are ω_t^{ref} and $|\lambda|^{\text{ref}}$. The MPP is parameterized by the optimal turbine speed at each wind speed, as estimated by the ES loop. The other control input, $|\lambda|^{\text{ref}}$, defines the level of the flux linkage of the rotor which prevents induction generator from magnetic saturation.

Combination of the Controller and WECS results in fast dynamics, while the dynamics contained in the ES algorithm are of slow and medium speeds. The algorithm estimates the optimal turbine speed, $\omega_t^{\text{ref}} = \omega_t^*$. With respect to the controller-system's fast dynamics, this can be considered a constant value.

Simulation Results on a WECS Model

A time frame of 30 seconds demonstrates the differences between the proposed algorithm and that of the conventional MPPT which is based on P&O with an FOC in the inner loop. The MPPT process is shown in **Figure 6**. The extracted energy by our proposed algorithm is 2.36% higher than the extracted energy by the conventional MPPT and FOC. Our algorithm provides perfect input-output decoupling and guarantees a larger domain of attraction, which increases performance robustness with respect to the system parameters. The improved efficiency also increases the competitiveness of wind energy.

PHOTOVOLTAIC SYSTEMS

Extremum seeking has been applied to MPPT design for photovoltaic (PV) micro-converter systems, where each PV module is coupled with its own DC/DC converter. Most existing MPPT designs are distributed (decentralized), i.e., they employ one MPPT loop around each converter, and all designs, whether distributed or multivariable, are gradient-based₂. The convergence rate of gradient-based designs depends on the Hessian, which in turn is dependent on environmental conditions such as irradiance and temperature. Consequently, when applied to large PV arrays, the variability in conditions, and/or PV module degradation, results in non-uniform transients in the convergence to the MPP. Using a multivariable gradient-based ES algorithm for the entire system instead of a scalar one for each PV module, decreases sensitivity to the Hessian, but does

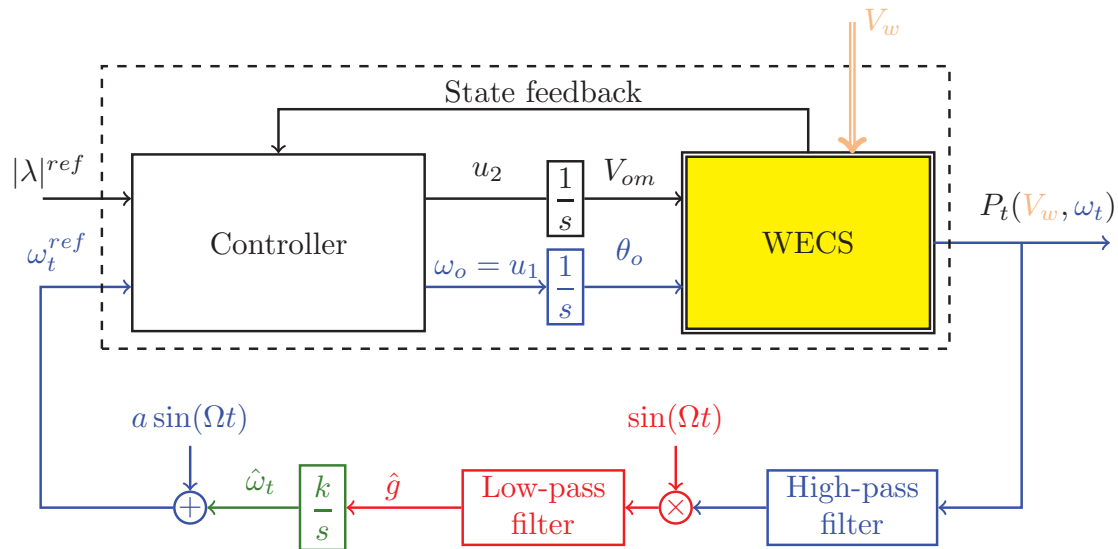


FIGURE 5 The ES algorithm for MPPT of the WECS with the inner-loop control.

not eliminate this dependence. The Newton-based ES algorithm is used, as it simultaneously employs estimates of the gradient and Hessian in the peak power tracking. The convergence rate of such a design to the MPP is independent of the Hessian, with tunable transient performance that is independent of environmental conditions. Experimental results demonstrate the effectiveness of the proposed algorithm in comparison to existing scalar designs, as well as multivariable, gradient-based ES.

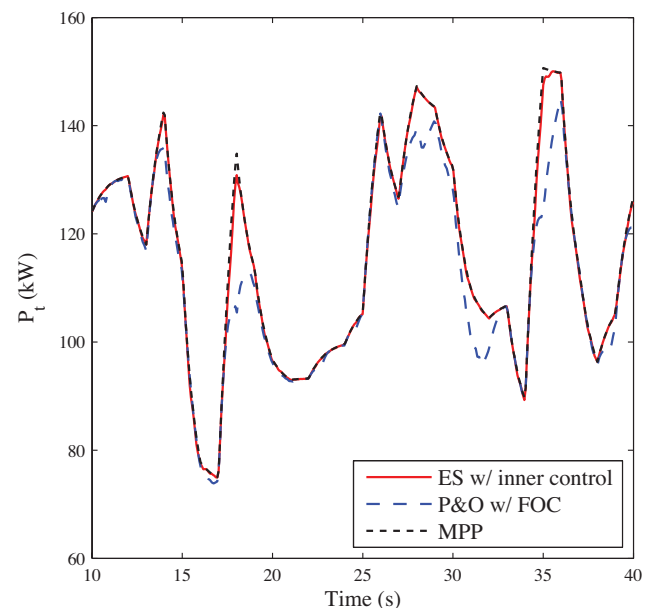
Using a multivariable gradient-based ES MPPT design for the micro-converter architecture, where each PV module is coupled with its own DC/DC converter, reduces the number of required sensors (hardware reduction). Transients under sudden changes in solar irradiance are more uniform as is the environmental temperature in comparison to a scalar gradient-based ES for each PV module. True of gradient-based designs, the convergence to MPP is dependent on the unknown Hessian: it varies with irradiance, temperature, and module degradation and mismatch.

In comparison with the standard gradient-based multivariable extremum seeking, the Newton-based ES removes the dependence of the convergence rate on the unknown Hessian and makes the convergence rate of the parameter estimates user-assignable. In particular, all the parameters can be designed to converge with the same speed, yielding straight trajectories to the extremum even with maps that have highly elongated level sets. When applied to the MPPT problem in PV systems, the method offers the benefit of uniform convergence behavior under a wide range of working conditions that includes temperature and irradiance variations and the non-symmetric power generation of the neighboring PV modules as a result of module degradation or mismatch.

FIGURE 6 Proposed algorithm, MPPT (solid red); conventional P&O with FOC (dashed blue); maximum power available to the WECS (dashed black).

Multivariable MPPT of PV Systems

Conventionally, each DC/DC converter has a MPPT loop to extract maximum power from the PV system (known as power optimizer in industry). The output sides of the converters are connected in series. The PV system is connected to the power grid through a DC/AC inverter, which has its separate controller. Two problems arise here. First, two sensors, current and voltage, are required per module which increase the levelized energy cost. Second, the coupling effect between PV modules is not addressed by this distributed control.



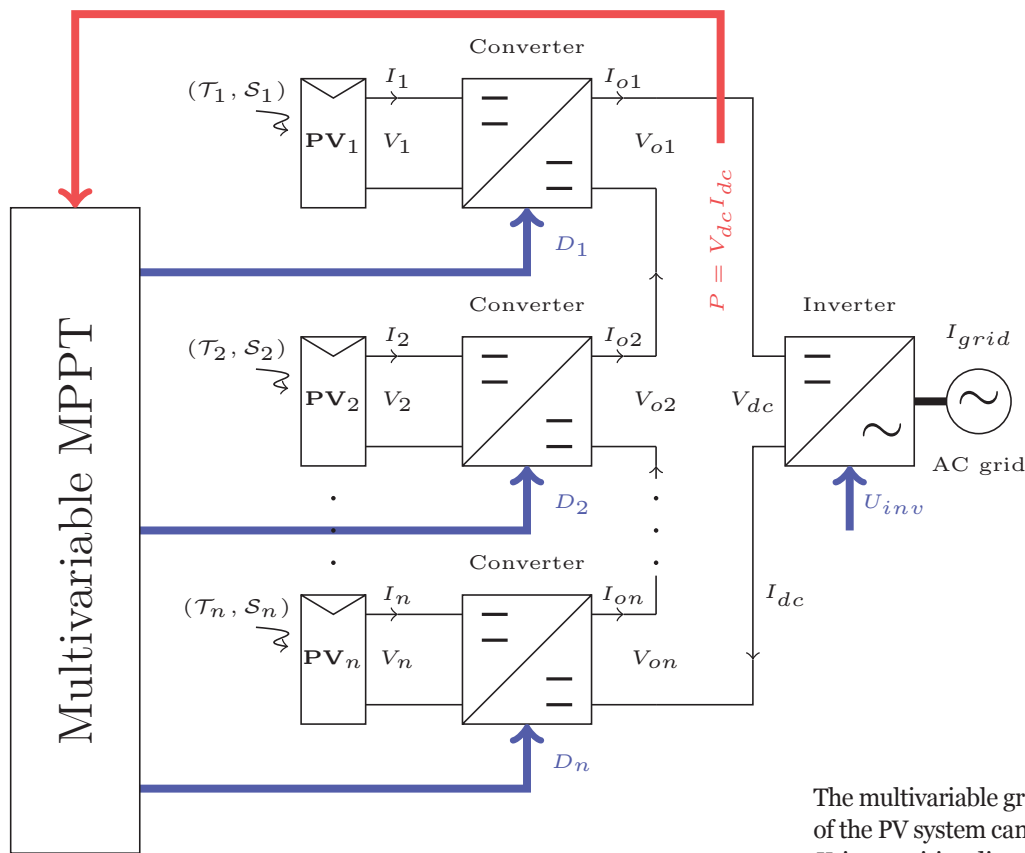


FIGURE 7 Multivariable MPPT for a PV system. One MPPT is used for the entire system. Temperature, and irradiance, vary all over the modules.

Figure 7 presents a multivariable MPPT based on an ES scheme with the following features:

- As it is applied to micro-converter systems, characterized by non-unimodal power, the design specializes in the issue of module mismatch—for example, different irradiance levels as a result of partially shaded conditions.
- The use of the non-model-based ES technique enables the design to respond robustly even with partial knowledge of system parameters and operating conditions.
- More efficient and cost-effective than a scalar design, the multivariable model requires just 2 sensors—one for the overall PV system current, and another for DC bus voltage—a significant hardware cost reduction.
- Interactions between PV modules are inherent to the multivariable design, so the transient performance is less sensitive to variations in environmental conditions than a corresponding scalar model.

Gradient-Based ES

Maximizing the power generated by all PV modules is equal to

$$P = \sum_{i=1}^n P_i = V_{dc} I_{dc}. \quad 10$$

For a micro-converter structure including n PV modules in cascade connection, there exists $D^* \in \mathbb{R}^n$ such that

$$\frac{\partial P}{\partial D}(D^*) = 0, \quad \frac{\partial^2 P}{\partial D^2}(D^*) = H < 0, \quad H = H^T. \quad 11$$

The multivariable gradient-based ES design to MPPT of the PV system can be used in Fig. 7. The ES gain, K , is a positive diagonal matrix, and the perturbation signals are defined as equations 2 and 3.

In particular, the design derives an estimate \hat{G} of the gradient vector by adding the “probing signal” $S(t)$ to the estimate $\hat{D} = [\hat{D}_1, \hat{D}_2, \dots, \hat{D}_n]^T$ of the pulse duration vector (of all the DC/DC converters). With no additional information on the Hessian (and also for simplicity), we choose the amplitudes of the probing signals to all be the same value a . It can be shown that for a proper set of ES parameters and with $K > 0$, the estimate \hat{D} of the pulse duration vector and the output P settle in a small ball around the optimal pulse duration $D^* = [D_1^*, D_2^*, \dots, D_n^*]^T$ and the MPP $P(D^*)$, respectively. The lowest probing frequency and its corresponding amplitude define the radius of the ball.

Since the cost function P varies with irradiance, temperature, and degradation of the PV modules, so does H , and therefore a fixed adaptation gain K results in different (condition dependent) convergence rates for each converter. In order to alleviate the issue of unknown Hessian dependent convergence, we present in the next section a modified version of the multivariable Newton-based ES. The Newton-based algorithm makes the convergence rate of the parameter estimates user-assignable. In particular, all the parameters can be designed to converge with the same speed, yielding straight trajectories to the extremum even with maps that have highly elongated level sets. When applied to

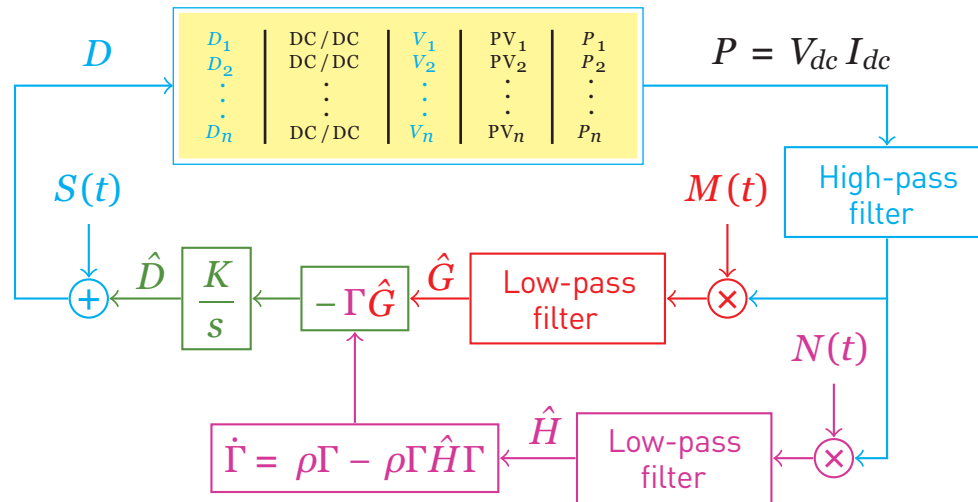


FIGURE 8 Multivariable Newton-based ES for MPPT of a PV system. The purple part is added to the gradient-based ES to estimate the Hessian.

the MPPT problem in PV systems, the method offers the benefit of uniform convergence behavior, under a wide range of working conditions that include temperature and irradiance variations, and under the non-symmetric power generation of the neighboring PV modules as a result of module degradation or mismatch.

Newton-Based ES

The multivariable Newton-based ES that we propose is shown schematically in **Figure 8**. As is clear from the figure, the proposed scheme extends the gradient-based ES with the estimate of the Hessian. The perturbation matrix is defined as equation 5.

The goal of the Newton-based design is to replace the estimation-error dynamics $\dot{\tilde{D}} = KH\tilde{D}$ with one of the form $\dot{\tilde{D}} = -KIH\tilde{D}$, where $\Gamma = H^{-1}$, that removes the dependence on the Hessian H . Calculating Γ (estimate of H^{-1}) in an algebraic fashion creates difficulties when \hat{H} is close to singularity or is indefinite. To deal with this problem, a dynamic estimator is employed to calculate the inverse of \hat{H} using a Riccati equation.

Consider the following filter

$$\dot{\mathcal{H}} = -\rho\mathcal{H} + \rho\hat{H} \quad 12$$

Note that the state of this filter converges to \hat{H} , an estimate of H . Denote $\Gamma = H^{-1}$. Since $\dot{\Gamma} = -\Gamma\dot{H}\Gamma$, then equation 12 is transformed into the differential Riccati equation

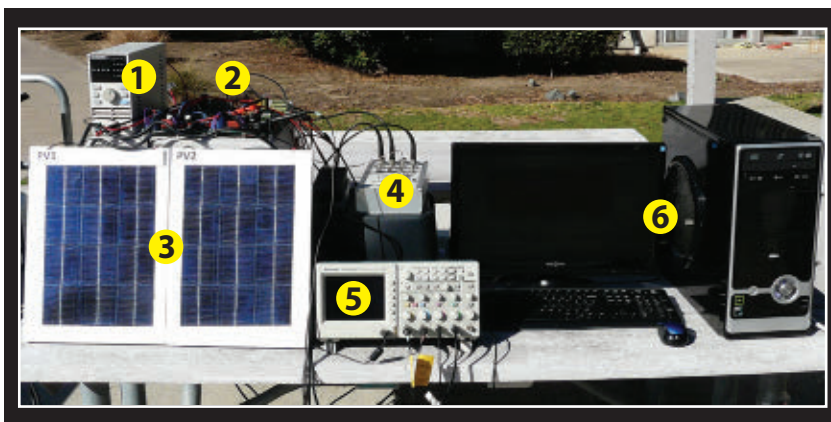
$$\dot{\Gamma} = \rho\Gamma - \rho\Gamma\hat{H}\Gamma. \quad 13$$

After a transient, the Riccati equation converges to the actual value of the inverse of Hessian matrix if \hat{H} is a good estimate of H .

The convergence rate of the parameter is independent of the shape of the cost function, and consequently, after transient, when the Hessian is close enough to its actual value, the output power converges to the MPP with the same performance regardless of environmental or mismatch conditions.

FIGURE 9 Experimental setup.

- | | |
|-----------------------------|--------------------------------------|
| 1 DC Bus | 4 CP 1104 |
| 2 DC/DC Converters, 1 and 2 | 5 Oscopce |
| 3 PV Panels, 1 and 2 | 6 DS 1104, Simulink and Control Desk |



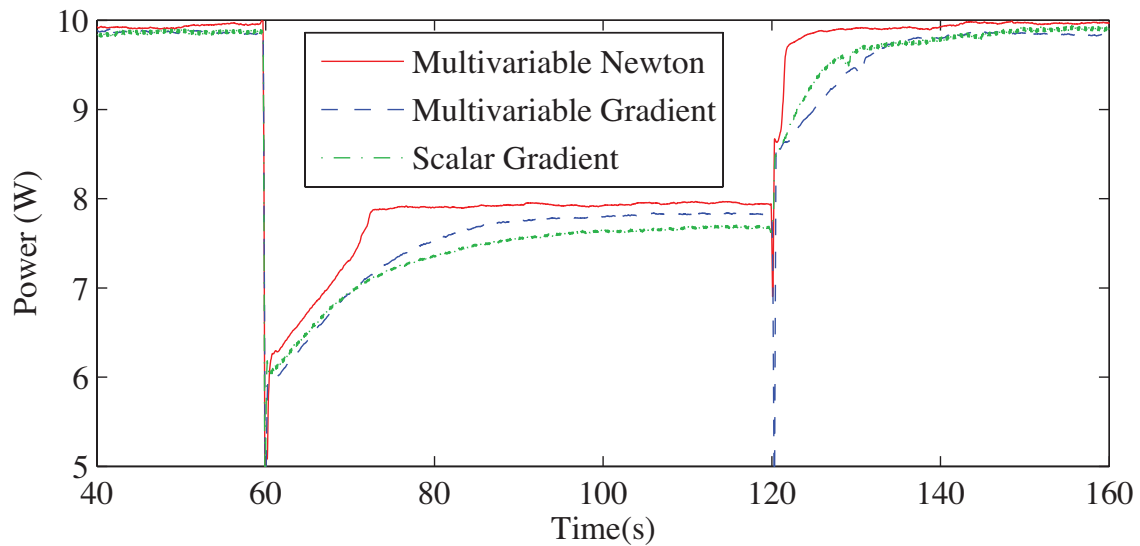


FIGURE 10 Variation of power versus time. The Newton algorithm shows uniform and fast transient with low steady-state error.

Experimental Results

To show the effectiveness of the proposed Newton-based design in Fig. 8, and compare its performance with that of the gradient-based design, we present experimental results for a PV system with $n = 2$ cascade modules. The physical hardware setup is shown in **Figure 9**. The temperature of PV modules is $25\text{ }^{\circ}\text{C}$ and the modules are fully exposed to the sun between 0-60 s and 120-180 s. To simulate the effect of partial shading, PV1 is covered with a plastic mat from time 60-120 s. When one module is partially shaded the overall power level decreases. We not only compare the multivariable gradient-based and Newton-based designs, but also the traditional scalar gradient-based design, that has one MPPT loop for each converter.

Figure 10 shows the performance of the 3 designs, and it is clear that the Newton algorithm recovers from this power level change faster than the other 2 algorithms. While the Newton method has the least steady-state error and uniform response under step down and step up power scenarios, the scalar design has the highest steady-state error and large response time in face of power decrease. The multivariable gradient-based ES performs better than the scalar MPPT under partial shading conditions.

The irradiance level of the partially shaded module is returned to normal level at $t = 120$ s. At this point the Newton scheme shows faster transient in comparison to the similar transient of the multivariable gradient-based ES and the distributed ES. The results demonstrate that the convergence rate of the Newton scheme does not vary largely from step up to step down in power generation, which is not true for the gradient-based and distributed MPPT schemes. Not surprisingly, the experimental results are in keeping with the analytical results.

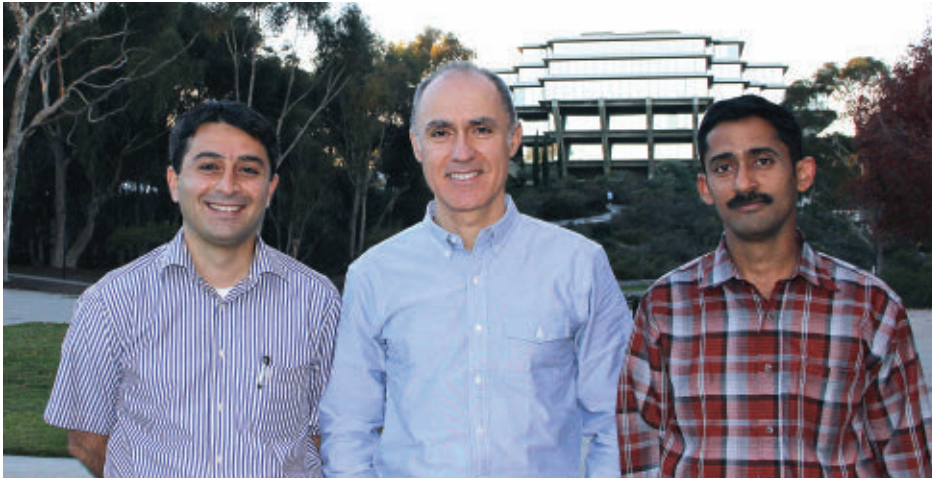
CONCLUDING REMARKS

Since environmental parameters like solar irradiance and wind speed affect the power map and maximum power point (MPP) of photovoltaic

(PV) and wind energy conversion systems (WECS), we propose extremum-seeking (ES), which is a model-free real-time optimization algorithm, for maximum energy harvest or maximum-power-point-tracking (MPPT) in such systems.

Extremum seeking is effective at guiding the WECS to its MPP in the sub-rated power region. However, the open-loop dynamics of the WECS have slow left half-plane poles that make the response time of the ES even slower. In order to achieve fast closed-loop response and extra features like constant voltage-to-frequency or vector control in the system, we design an inner-loop control based on the field-oriented control (FOC) concept. The combination of the inner-loop controller and the ES algorithm improves the performance of the WECS, as shown by the simulations.

For PVs, we consider the micro-converter architecture, where each module is connected to its own DC-DC converter. Conventional designs are scalar. First, they ignore the interaction between modules, and secondly, they require two (sensor) measurements per module. A multivariable design that improves on each of these aspects is



Left to right: Azad Ghaffari, Miroslav Krstic, and Sridhar Seshagiri.

ABOUT THE AUTHORS

Azad Ghaffari received his B.S. degree in Electrical Engineering and M.S. degree in Control Engineering from K.N. Toosi University of Technology in Tehran, Iran. He received his PhD degree in Mechanical and Aerospace Engineering from the Joint Doctoral Program between San Diego State University and University of California, San Diego. His research interests include demand response in power systems, extremum seeking and its application to maximum power point tracking in photovoltaic and wind energy conversion systems, induction machines, power electronics, and sliding mode control.

Miroslav Krstic is the Alspach endowed chair professor at UCSD, founding director of the Cymer Center for Control Systems and Dynamics and Associate Vice Chancellor for Research. Krstic is a recipient of PECASE, NSF Career, ONR Young Investigator, Axelby, Schuck,

and UCSD Research award, and is a Fellow of IEEE and IFAC. He has held Springer-Berkeley and Royal Academy of Engineering distinguished visiting professorships. He has served as Senior Editor of *IEEE TAC* and *Automatica*, VP of CSS, and chair of its IEEE Fellow Committee. Krstic is coauthor of ten books on nonlinear, adaptive, PDE control, and delay systems.

Sridhar Seshagiri received his B.S. Tech degree from the Indian Institute of Technology, Madras, and his M.S. and Ph.D degrees from Michigan State University, in 1995, 1998, and 2003 respectively, all in electrical engineering. He joined the Electrical & Computer Engineering Department at San Diego State University in 2003, where he is currently an Associate Professor. His research interests are nonlinear control with applications to energy systems.

REFERENCES

- 1 Draper, C. S., and Li, Y. T., "Principles of Optimizing Control Systems and an Application to the Internal Combustion Engine," *Optimal and Self-Optimizing Control*, M.I.T. Press, 1951
- 2 Eram, T., and Chapman, "Comparison of photovoltaic array maximum power point tracking techniques," *IEEE Transactions on Energy Conversion*, vol. 22, pp. 439–449, 2007.
- 3 Krstic, M., and Wang, H.-H., "Stability of extremum seeking feedback for general nonlinear dynamic systems," *Automatica*, vol. 36, pp. 595–601, 2000.
- 4 Ariyur, K. B., and Krstic M., *Real-Time Optimization by Extremum Seeking Feedback*, Wiley-Interscience, 2003.
- 5 Tan, Y., Netic, D., and Mareels, I., "On non-local stability properties of extremum seeking control," *Automatica*, vol. 42, pp. 889–903, 2006.
- 6 Liu, S.J., and Krstic, M., *Stochastic Averaging and Stochastic Extremum Seeking*, Springer, 2012.
- 7 Ghaffari, A., Krstic, M., and Netic, D., "Multivariable Newton-based extremum seeking," *Automatica*, vol. 48, pp. 1759–1767, 2012.

proposed. A multivariable gradient-based ES algorithm was considered first, where the Hessian of the power map has a dominant role in the closed-loop performance. Next, a Newton-based ES algorithm was employed, which removed the performance dependence of the gradient-based design on the Hessian. The Newton-based design has two distinguishing components that are key: a perturbation matrix that

generates the estimate of the Hessian, and a dynamic filter that estimates the inverse of the Hessian. Experimental results verify the effectiveness of the Newton-based MPPT, versus its scalar and multivariable gradient-based counterparts. ■